Acta of Bioengineering and Biomechanics
Vol. 10, No. 2, 2008

The modelling of heating a tissue subjected to external electromagnetic field

EWA MAJCHRZAK*, GRZEGORZ DZIATKIEWICZ, MAREK PARUCH

Department for Strength of Materials and Computational Mechanics, Silesian University of Technology,
Konarskiego 18A, 44-100 Gliwice, Poland.
E-mail: grzegorz.dziatkiewicz@polsl.pl, marek.paruch@polsl.pl

The boundary element method (BEM) is used to solve the coupled problem connected with the biological tissue heating. The tissue treated as a non-homogeneous domain (healthy tissue and tumor region) is subjected to external electromagnetic field. The thermal effect is produced by electrodes that touches the skin surface. External electromagnetic field generates the internal temperature field, which can be modelled by using the volumetric internal heat sources in the tissue domain (this source function constitutes one of components of the Pennes equation). In the paper, both BEM application to coupled bioheat transfer problems and numerical results of computations are theoretically considered. The successive examples show the different input data determining the electromagnetic field parameters.

Key words: *biological tissue heating, bioheat transfer modelling, electromagnetic field*

1. Introduction

Hyperthermia occurs when the body produces or absorbs more heat than it can dissipate. This is usually due to excessive exposure to heat. Hyperthermia can also be produced artificially by medical devices and it may be used as a therapeutic method to bring about an artificial rise in temperature in certain types of cancer tissues, such as skin cancer [1]. Up to now, various heating methods allowing hyperthermia to be produced, such as resistive heating with external electrodes [1]–[3], microwaves [4], [5], ultrasound [6] and lasers [7], have been used. It has been well established that the temperature above 42 °C causes necrosis of living cells. The heat has to be applied directly to the tumor in order to prevent the damage to healthy tissue surrounding the tumor. The knowledge of the entire temperature field in the treatment region allows us to control the tumor heating.

The paper deals with the modelling of biological tissue heating by external electromagnetic field. To analyse the problem a simplified 2D mathematical model based on the Pennes equation supplemented with an equation determining the electric field produced by the external electrodes is built; at the same time different values of electric field parameters have been taken into account. The model has been subjected to the numerical investigations using the boundary element method. It should be pointed out that the temperature differences and temperature gradients in the domain considered are rather small. The BEM guarantees a high accurracy of numerical simulation (due to a good approximation of boundary conditions), but it is not popular as a tool for solving the bioheat transfer problems. The algorithm, numerical procedures in the case of non-homogeneous domain, and also the adequate computer program have been designed by the authors of this paper. Our main objective was to develop the boundary element method

* Corresponding author: Ewa Majchrzak, Silesian University of Technology, ul. Konarskiego 18a, 44-100 Gliwice, Poland, e-mail: ewa.majchrzak@polsl.pl
Received: March 26, 2008
Accepted for publication: June 9, 2008

that can be applied to coupled problems connected with bioheat transfer modelling.

2. Governing equations

In figure 1, a typical radio-frequency (RF) hyperthermia system is shown [2]. The mathematical model of the process analyzed consists of two parts [2], [3]. In the electromagnetic part, the electric field distribution is obtained based on the Laplace equation. The thermal part is connected with the bioheat transfer equation to obtain a temperature distribution. In the bioheat transfer equation, an additional source term associated with the heat generation caused by electric field distribution appears.

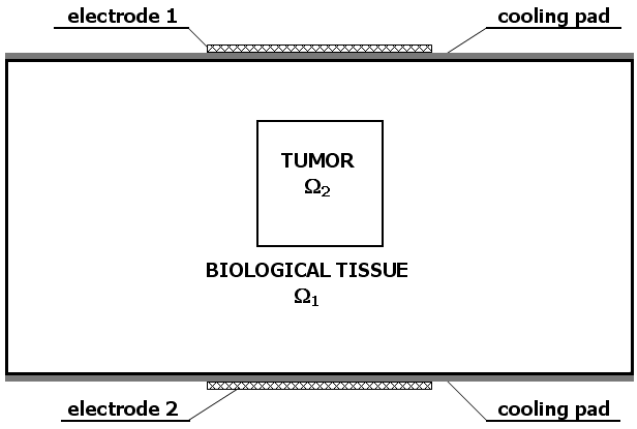

Fig. 1. Hyperthermia system

Because the wavelength of the RF current in tissues is much greater compared to the depth of a human body, the quasistatic electric field approximation can be applied. The quasistatic electric field is irrotational, so the electric potential can be introduced. The electric potential $\varphi_1(x, y)$ inside the healthy tissue Ω_1 is described by the Laplace equation

$$(x, y) \in \Omega_1 : \quad \nabla[\varepsilon_1(x, y)\varphi_1(x, y)] = 0\,, \tag{1}$$

where $\varepsilon_1(x, y)$ [$C^2/(Nm^2)$] is the dielectric permittivity of tissue.

The electric potential $\varphi_2(x, y)$ inside the tumor Ω_2 is described by a similar equation

$$(x, y) \in \Omega_2 : \quad \nabla[\varepsilon_2(x, y)\varphi_2(x, y)] = 0\,, \tag{2}$$

where $\varepsilon_2(x, y)$ is the dielectric permittivity of tumor.

At the interface Γ_c between the tumor and healthy tissue (figure 2) the ideal electric contact is assumed

$$(x, y) \in \Gamma_c : \begin{cases} \varphi_1(x, y) = \varphi_2(x, y), \\ -\varepsilon_1 \dfrac{\partial \varphi_1(x, y)}{\partial n} = -\varepsilon_2 \dfrac{\partial \varphi_2(x, y)}{\partial n}. \end{cases} \tag{3}$$

On the external surface of tissue being in contact with the electrodes the following conditions are accepted

$$\begin{aligned} &(x, y) \in \Gamma_1 : \quad \varphi_1(x, y) = U, \\ &(x, y) \in \Gamma_2 : \quad \varphi_2(x, y) = -U, \end{aligned} \tag{4}$$

where U [V] is the electric potential of the electrode relative to the ground.

On the remaining external boundary of the tissue, the ideal electric isolation is assumed:

$$(x, y) \in \Gamma_3 \cup \Gamma_4 \cup \Gamma_5 \cup \Gamma_6 \cup \Gamma_7 \cup \Gamma_8 :$$

$$-\varepsilon_1 \frac{\partial \varphi_1(x, y)}{\partial n} = 0. \tag{5}$$

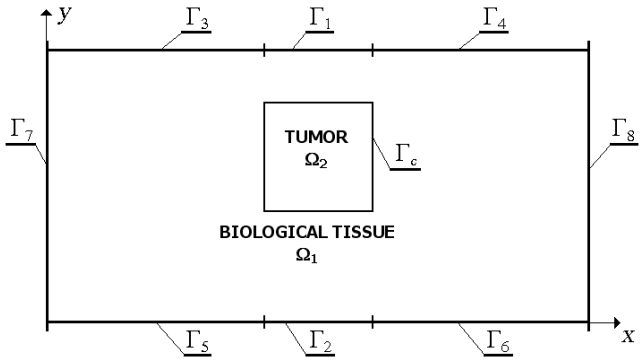

Fig. 2. Domain of tissue with a tumor

The electric field inside the tissue is described by the following equation

$$\mathbf{E}_e(x, y) = -\nabla \varphi_e(x, y) = -\begin{bmatrix} \dfrac{\partial \varphi_e(x, y)}{\partial x} \\ \dfrac{\partial \varphi_e(x, y)}{\partial y} \end{bmatrix}. \tag{6}$$

Heat generation Q_e [W/m^3] due to the electromagnetic power dissipated in healthy tissue ($e = 1$) and tumor region ($e = 2$) depends on the conductivity σ_e [S/m] and the electric field **E** [2]

$$\begin{aligned} Q_e(x, y) &= \frac{\sigma_e |\mathbf{E}_e(x, y)|}{2} \\ &= \frac{\sigma_e}{2}\left[\left(\frac{\partial \varphi_e(x, y)}{\partial x}\right)^2 + \left(\frac{\partial \varphi_e(x, y)}{\partial y}\right)^2\right]. \end{aligned} \tag{7}$$

The temperature field in the healthy tissue and the tumor region is described by the system of the Pennes equations [2], [8]–[10]

$$(x, y) \in \Omega_e : \lambda_e \nabla^2 T_e(x, y) + G_{Be} c_B [T_B - T_e(x, y)] + Q_{\text{mete}} + Q_e(x, y) = 0, \quad (8)$$

where $e = 1$ and $e = 2$ correspond to the healthy tissue and tumor region, respectively, T_e denotes the temperature, λ_e [W/(mK)] is the thermal conductivity, G_{Be} [1/s] is the perfusion rate, c_B [J/(m^{3}K)] is the volumetric specific heat of blood, T_B is the temperature of blood supplying arteries which is treated as a constant, Q_{mete} [W/m^3] is the metabolic heat source.

At the interface Γ_c between the tumor and healthy tissue an ideal contact is accepted

$$(x, y) \in \Gamma_c : \begin{cases} T_1(x, y) = T_2(x, y), \\ -\lambda_1 \dfrac{\partial T_1(x, y)}{\partial n} = -\lambda_2 \dfrac{\partial T_2(x, y)}{\partial n}. \end{cases} \quad (9)$$

On the upper and lower surfaces of healthy tissue domain (skin surface) the convection condition is assumed [2]

$$\Gamma_1 \cup \Gamma_2 \cup \Gamma_3 \cup \Gamma_4 \cup \Gamma_5 \cup \Gamma_6 : -\lambda_1 \frac{\partial T_1(x, y)}{\partial n} = \alpha_w [T_1(x, y) - T_w], \quad (10)$$

where α_w [W/(m^{2}K)] is the coefficient of heat transfer between the skin surface and the cooling water, T_w is the cooling water temperature. At a stage of numerical simulation the Dirichlet condition in place of (10) can also be considered. If $\alpha_w \to \infty$ then $T_1(x, y) \to T_w$. So, introducing into the set of input data the value α_w that equals, e.g., 10^{12}, one arrives at the solution corresponding to the Dirichlet boundary condition. Summing up, using the same computer program, the different types of boundary conditions on skin surface [11] can be considered. On the boundaries Γ_7, Γ_8 the adiabatic condition $-\lambda \partial T_1/\partial n = 0$ can be taken into account. This condition results from the consideration that in the positions far from the center of the domain, the temperature field is almost not affected by the external heating [2].

3. Boundary element method

In order to solve the equations describing the potential of electric field and the temperature field in the domain considered, the boundary element method has been applied [9], [14], [15]. The boundary integral equations corresponding to equations (1), (2) can be expressed by:

$$B_e(\xi, \eta)\varphi_e(\xi, \eta) + \int_\Gamma \psi_e(x, y)\varphi_e^*(\xi, \eta, x, y)d\Gamma = \int_\Gamma \varphi_e(x, y)\psi_e^*(\xi, \eta, x, y)d\Gamma, \quad e = 1, 2, \quad (11)$$

where (ξ, η) is the observation point, the coefficient $B_e(\xi, \eta)$ depends on the location of the source point (ξ, η) and $\psi_e(x, y) = -\varepsilon_e \partial \varphi_e(x, y)/\partial n$. In the domain Ω_1, the boundary Γ corresponds to the external and internal boundaries of healthy tissue; in the domain Ω_2, the boundary Γ is denoted by Γ_c as shown in figure 2. Fundamental solution of the problem discussed has the following form

$$\varphi_e^*(\xi, \eta, x, y) = \frac{1}{2\pi\varepsilon_e} \ln \frac{1}{r}, \quad (12)$$

where r is the distance between the points (ξ, η) and (x, y). Differentiating the function $\varphi_e^*(\xi, \eta, x, y)$ with respect to the outward normal $\mathbf{n} = [\cos\alpha, \cos\beta]$, the function $\psi_e^*(\xi, \eta, x, y)$ is obtained

$$\psi_e^*(\xi, \eta, x, y) = -\varepsilon_e \frac{\partial \varphi_e^*(\xi, \eta, x, y)}{\partial n} \frac{d}{4\pi r^2}, \quad (13)$$

where

$$d = (x - \xi)\cos\alpha + (y - \eta)\cos\beta. \quad (14)$$

The boundaries of the domains are divided into N_1 and N_2 boundary elements, respectively, as shown in figure 3.

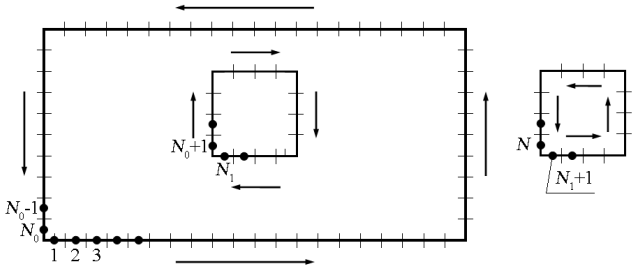

Fig. 3. Boundary elements and nodes

For constant boundary element, it is assumed that

$$(x, y) \in \Gamma_j : \begin{cases} \varphi_e(x, y) = \varphi_e(x_j, y_j) = \varphi_j^e, \\ \psi_e(x, y) = \psi_e(x_j, y_j) = \psi_j^e, \end{cases} \quad (15)$$

and then the following approximation of equation (11) can be obtained:

- for healthy tissue

$$\sum_{j=1}^{N_0} G_{ij}^1 \psi_j^1 + \sum_{j=N_0+1}^{N_1} G_{ij}^1 \psi_j^1 = \sum_{j=1}^{N_0} H_{ij}^1 \varphi_j^1 + \sum_{j=N_0+1}^{N_1} H_{ij}^1 \varphi_j^1, \quad i = 1, 2, ..., N_1; \tag{16}$$

- for tumor region

$$\sum_{j=N_1+1}^{N} G_{ij}^2 \psi_j^2 = \sum_{j=N_1+1}^{N} H_{ij}^2 \varphi_j^2, \quad i = N_1 + 1,\ N_1 + 2, ..., N\ , \tag{17}$$

where

$$G_{ij}^e = \int_{\Gamma_j} \varphi_e^*(\xi_i, \eta_i, x, y) d\Gamma_j, \quad e = 1, 2 \tag{18}$$

and

$$H_{ij}^e = \int_{\Gamma_j} \psi_e^*(\xi_i, \eta_i, x, y) d\Gamma_j, \quad e = 1, 2, \tag{19}$$

while $H_{ii}^e = -0.5$.

The boundary condition (3) on the contact surface (healthy tissue – tumor region) written in the form of:

$$\begin{cases} \varphi_j^1 = \varphi_j^2 = \varphi_j, \\ \psi_j^1 = -\psi_j^2 = \psi_j \end{cases} \tag{20}$$

is introduced into the systems of equations (16), (17). Hence, one obtains

$$\sum_{j=1}^{N_0} G_{ij}^1 \psi_j + \sum_{j=N_0+1}^{N_1} G_{ij}^1 \psi_j = \sum_{j=1}^{N_0} H_{ij}^1 \varphi_j + \sum_{j=N_0+1}^{N_1} H_{ij}^1 \varphi_j, \quad i = 1, 2, ..., N_1 \tag{21}$$

and

$$-\sum_{j=N_1+1}^{N} G_{ij}^2 \psi_j = \sum_{j=N_1+1}^{N} H_{ij}^2 \varphi_j, \quad i = N_1 + 1,\ N_1 + 2, ..., N, \tag{22}$$

or using matrix convection, one arrives at

$$[\mathbf{G}^1 \ \ \mathbf{G}_c^1] \begin{bmatrix} \boldsymbol{\psi}^1 \\ \boldsymbol{\psi} \end{bmatrix} = [\mathbf{H}^1 \ \ \mathbf{H}_c^1] \begin{bmatrix} \boldsymbol{\varphi}^1 \\ \boldsymbol{\varphi} \end{bmatrix} \tag{23}$$

and

$$-\mathbf{G}_c^2 \boldsymbol{\psi} = \mathbf{H}_c^2 \boldsymbol{\varphi}\ . \tag{24}$$

Joining together the systems of equations (23), (24), one has

$$\begin{bmatrix} \mathbf{G}^1 & -\mathbf{H}_c^1 & \mathbf{G}_c^1 \\ \mathbf{0} & -\mathbf{H}_c^2 & -\mathbf{G}_c^2 \end{bmatrix} \begin{bmatrix} \boldsymbol{\psi}^1 \\ \boldsymbol{\varphi} \\ \boldsymbol{\psi} \end{bmatrix} = \begin{bmatrix} \mathbf{H}^1 \boldsymbol{\varphi}^1 \\ \mathbf{0} \end{bmatrix}. \tag{25}$$

Then, the remaining boundary conditions (4), (5) should be introduced into the system of equations (25). This system allows the "missing" boundary values of the functions φ_j^e, ψ_j^e to be determined.

It should be pointed out that in order to determine the electric field inside the tissue (equation (6)), the partial derivatives $\partial\varphi_e(x, y)/\partial x$, $\partial\psi_e(x, y)/\partial y$ have to be known. One of the possibilities is making use of equations (11) for internal nodes $(\xi, \eta)(B_e(\xi, \eta) = 1)$ and then of the following relationships:

$$\frac{\partial \varphi_e(\xi,\eta)}{\partial \xi} = \int_\Gamma \varphi_e(x,y) \frac{\partial \psi_e^*(\xi,\eta,x,y)}{\partial \xi} d\Gamma - \int_\Gamma \psi_e(x,y) \frac{\partial \varphi_e^*(\xi,\eta,x,y)}{\partial \eta} d\Gamma \tag{26}$$

and

$$\frac{\partial \varphi_e(\xi,\eta)}{\partial \eta} = \int_\Gamma \varphi_e(x,y) \frac{\partial \psi_e^*(\xi,\eta,x,y)}{\partial \eta} d\Gamma - \int_\Gamma \psi_e(x,y) \frac{\partial \varphi_e^*(\xi,\eta,x,y)}{\partial \xi} d\Gamma, \tag{27}$$

where

$$\frac{\partial \varphi_e^*}{\partial \xi} = \frac{x-\xi}{2\pi\varepsilon_e r^2}, \quad \frac{\partial \varphi_e^*}{\partial \eta} = \frac{y-\eta}{2\pi\varepsilon_e r^2} \tag{28}$$

and

$$\frac{\partial \psi_e^*}{\partial \xi} = \frac{1}{2\pi}\left[\frac{2(x-\xi)d}{r^4} - \frac{\cos\alpha}{r^2}\right], \quad \frac{\partial \psi_e^*}{\partial \eta} = \frac{1}{2\pi}\left[\frac{2(y-\eta)d}{r^4} - \frac{\cos\beta}{r^2}\right]. \tag{29}$$

Applying the previously presented discretization of the boundaries for the subdomains, it is possible to perform numerical calculations of partial derivatives. These derivatives are determined at the internal nodes shown in figure 4.

The Pennes equations (8) can be written in the form

$$(x,y)\in\Omega_e:\ \ \lambda_e\nabla^2 T_e(x,y)-k_e T_e(x,y)+Q^e(x,y)=0, \tag{30}$$

where

$$k_e=G_{Be}c_B,\ \ Q^e(x,y)=k_e T_e+Q_{\text{mete}}+Q_e(x,y). \tag{31}$$

The boundary integral equations corresponding to equations (30) can be expressed as follows

$$\begin{aligned}B_e(\xi,\eta)T_e(\xi,\eta)+\int_\Gamma q_e(x,y)T_e^*(\xi,\eta,x,y)d\Gamma\\ =\int_\Gamma T_e(x,y)q_e^*(\xi,\eta,x,y)d\Gamma\\ +\int_\Omega T_e^*(\xi,\eta,x,y)Q^e(x,y)d\Omega_e,\ \ e=1,2,\end{aligned} \tag{32}$$

where

$$T_e^*(\xi,\eta,x,y)=\frac{1}{2\pi\lambda_e}K_0\left(r\sqrt{\frac{k_e}{\lambda_e}}\right) \tag{33}$$

and

$$\begin{aligned}q_e^*(\xi,\eta,x,y)&=-\lambda_e\frac{\partial T_e^*(\xi,\eta,x,y)}{\partial n}\\ &=\frac{d}{2\pi r}\sqrt{\frac{k_e}{\lambda_e}}K_1\left(r\sqrt{\frac{k_e}{\lambda_e}}\right),\end{aligned} \tag{34}$$

while $q_e(x,y)=-\lambda_e\partial T_e(x,y)/\partial n$. In formulas (33), (34), $K_0(\cdot)$ and $K_1(\cdot)$ are the modified Bessel functions of the second kind, zero and the first order, respectively [15].

To solve equations (32), not only the boundary of the domains considered, but also their interior should be discretized as shown in figure 4.

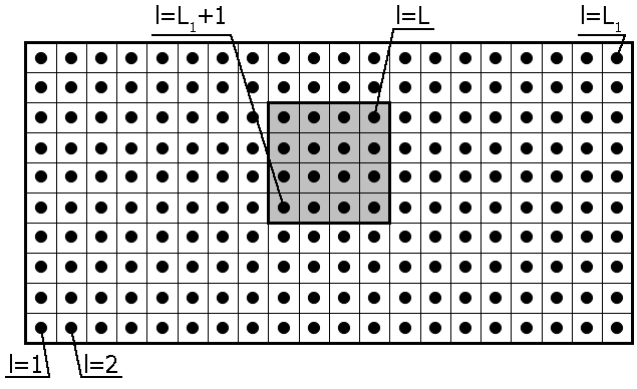

Fig. 4. Discretization of the subdomains considered

For constant boundary elements and constant internal cells one obtains the following systems of equations

- for healthy tissue

$$\begin{aligned}\sum_{j=1}^{N_0}W_{ij}^1q_j^1+\sum_{j=N_0+1}^{N_1}W_{ij}^1q_j^1\\ =\sum_{j=1}^{N_0}Z_{ij}^1T_j^1+\sum_{j=N_0+1}^{N_1}Z_{ij}^1T_j^1\\ +\sum_{l=1}^{L_1}P_{il}^1Q_l^1,\quad i=1,2,...,N_1;\end{aligned} \tag{35}$$

- for tumor region

$$\begin{aligned}\sum_{j=N_1+1}^{N}W_{ij}^2q_j^2=\sum_{j=N_1+1}^{N}Z_{ij}^2T_j^2+\sum_{l=L_1+1}^{L}P_{il}^2Q_l^2,\\ i=N_1+1,N_1+2,...,N,\end{aligned} \tag{36}$$

where

$$W_{ij}^e=\int_{\Gamma_j}T_e^*(\xi_i,\eta_i,x,y)d\Gamma_j,\quad e=1,2 \tag{37}$$

and

$$\begin{aligned}Z_{ij}^e=\int_{\Gamma_j}q_e^*(\xi_i,\eta_i,x,y)d\Gamma_j,\quad i\neq j,\\ Z_{ii}^e=-\frac{1}{2},\quad e=1,2,\end{aligned} \tag{38}$$

while

$$P_{il}^e=\int_{\Omega_l}T_e^*(\xi_i,\eta_i,x,y)d\Omega_l,\quad e=1,2. \tag{39}$$

The systems of equations (35) are coupled with boundary condition (9), which can be written as

$$\begin{cases}T_j^1=T_j^2=T_j,\\ q_j^1=-q_j^2=q_j.\end{cases} \tag{40}$$

Finally one obtains

$$\begin{bmatrix}\mathbf{W}^1 & -\mathbf{Z}_c^1 & \mathbf{W}_c^1\\ \mathbf{0} & -\mathbf{Z}_c^2 & -\mathbf{W}_c^2\end{bmatrix}\begin{bmatrix}\mathbf{q}^1\\ \mathbf{T}\\ \mathbf{q}\end{bmatrix}=\begin{bmatrix}\mathbf{Z}^1\mathbf{T}^1+\mathbf{P}^1\mathbf{Q}^1\\ \mathbf{P}^2\mathbf{Q}^2\end{bmatrix}. \tag{41}$$

The remaining boundary conditions should be introduced into the system of equations (41). The solution of (41) allows one to calculate the "missing" boundary temperatures T_j^e and heat fluxes q_j^e. Then the temperatures at the internal nodes are calculated based on the formulas

• for healthy tissue ($i = N + 1, N + 2, \ldots, N + L_1$)

$$T_i^1 = \sum_{j=1}^{N_1} Z_{ij}^1 T_j^1 - \sum_{j=1}^{N_1} W_{ij}^1 q_j^1 + \sum_{l=1}^{L_1} P_{il}^1 Q_l^1 ; \qquad (42)$$

• for tumor region ($i = N + L_1 + 1, N + L_1 + 2, \ldots, N + L$)

$$T_i^2 = \sum_{j=N_1+1}^{N} Z_{ij}^2 T_j^2 - \sum_{j=N_1+1}^{N} W_{ij}^2 q_j^2 + \sum_{l=L_1+1}^{L} P_{il}^2 Q_l^2 . \qquad (43)$$

In the paper, the external boundary of the tissue has been divided into 60 constant boundary elements, the interface Γ_c of the tumor and the tissue has been divided into 16 boundary elements. To solve the Pennes equation in the interiors of Ω_1 and Ω_2, the respective nodes (internal cells) $L_1 = 184$ and $L_2 = 16$ have been distinguished.

4. Results of computations

The rectangular domain of the dimensions of 0.08 m × 0.04 m has been considered. The heating area is described as $\{0.032 \text{ m} \le x \le 0.048 \text{ m}, y = 0\}$, $\{0.032 \text{ m} \le x \le 0.048 \text{ m}, y = 0.04 \text{ m}\}$, the tumor region corresponds to $\Omega_2 = \{0.032 \text{ m} \le x \le 0.048 \text{ m}, 0.016 \text{ m} \le y \le 0.032 \text{ m}\}$ as shown in figure 2.

At first, the temperature distribution in the tissue with tumor not exposed to electric field has been calculated. For healthy tissue the following parameters have been assumed: thermal conductivity $\lambda_1 = 0.5$ [W/(mK)], perfusion rate $G_{B1} = 0.0005$ [1/s], metabolic heat source $Q_{m1} = 4200$ [W/m^3], blood temperature $T_B = 37$ °C, volumetric specific heat of blood $c_B = 4.2$ [MJ/(m^{3}K)] [2]. It has been revealed that the presence of malignant tumor often leads to very different blood perfusion and abnormally high capacity of metabolic heat source in the tumor region [2], [8], [9]. The following parameters are thus given for a highly vascularized tumor diagnosed in the skin tissue: $G_{B2} = 0.002$ [1/s], $Q_{m2} = 42000$ [W/m^3], $\lambda_2 = 0.6$ [W/(mK)] [2]. Two variants of boundary conditions on skin surface have been taken into account. In the first variant the boundary temperature $T = 32.5$ °C has been assumed [12], [13] (figure 5), in the second one the convection boundary condition (equation (12): $\alpha_w = 45$ [W/(m^{2}K)], $T_w = 20$ °C) has been accepted (figure 6). The maximum temperatures in both cases, equal to 38.22 °C and 36.78 °C, respectively, have been achieved in the tumor region.

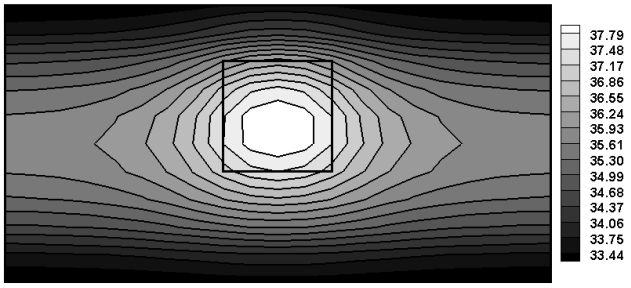

Fig. 5. Temperature distribution (without electromagnetic field) for the Dirichlet boundary condition on the skin surface ($T = 32.5$ °C)

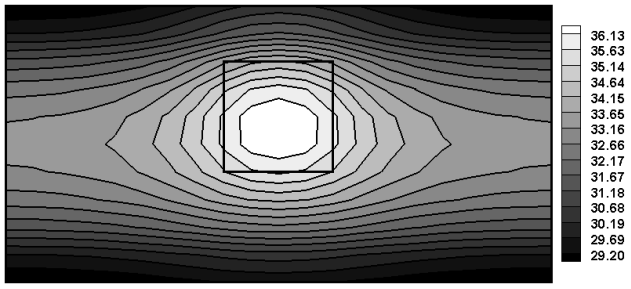

Fig. 6. Temperature distribution (without electromagnetic field) for convection boundary condition on the skin surface ($\alpha_w = 45$ [W/(m^{2}K)], $T_w = 20$ °C)

Table. Electric properties used for the calculations ($\varepsilon_0 = 8.85 \cdot 10^{-12}$ [C^2/(Nm^2)])

No.	Frequency f [MHz]	Dielectric permittivity [C^2/(Nm^2)]		Electrical conductivity [S/m]		Electric potential U [V]	Maximum temperature T [°C]
		ε_1	ε_2	σ_1	σ_2		
1	0.1	$20000\varepsilon_0$	$1.2\varepsilon_1$	0.192	$1.2\sigma_1$	5	37.44
2						10	39.42
3						15	42.80
4						20	49.38
5	1	$2000\varepsilon_0$	$1.2\varepsilon_1$	0.4	$1.2\sigma_1$	5	38.16
6						10	42.29
7						15	52.12
8						20	67.97
9	10	$100\varepsilon_0$	$1.2\varepsilon_1$	0.625	$1.2\sigma_1$	5	38.93
10						10	46.41
11						15	63.56
12						20	88.44

The aim of our investigations was to determine the parameters of electromagnetic field allowing the temperature in the tumor region to be higher than 42 °C. The input data introduced into the computer program are collected in the table [2]–[4]. In the last column, the maximum values of temperatures obtained for successive simulations are gathered (on the skin surface the convection condition has been assumed).

Even though the quasistatic electric field is assumed, the influence of electromagnetic wave frequency is also taken into account. Electric properties of human body tissues depend on the frequency (see the table). In figure 7, the electric field distribution for f = 10 [MHz] and U = 10 [V] is shown, while in figures 8, 9 the curves represent the derivatives $\partial\varphi(x, y)/\partial x$ and $\partial\varphi(x, y)/\partial y$. Then, on the basis of formula (7), the source function Q_e can be determined (figure 10). The temperature distribution corresponding to the case discussed is shown in figure 11.

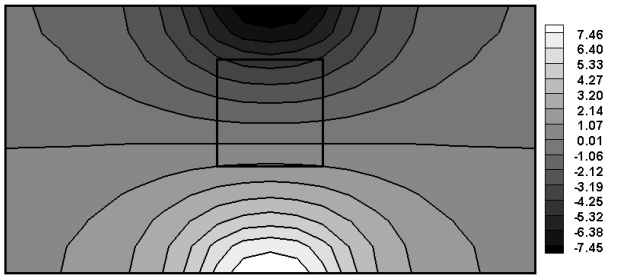

Fig. 7. Electric field distribution [V]
(f = 10 [MHz] and U = 10 [V])

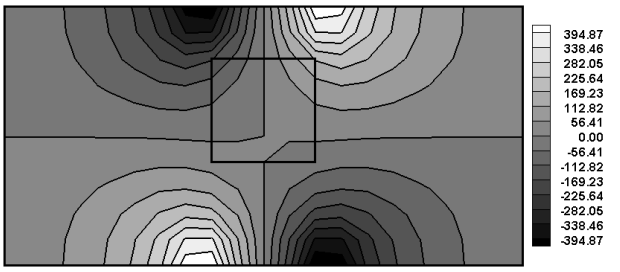

Fig. 8. Derivative $\partial\varphi(x, y)/\partial x$, [V/m]
(f = 10 [MHz] and U = 10 [V])

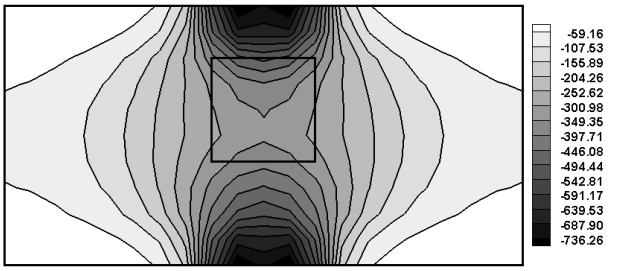

Fig. 9. Derivative $\partial\varphi(x, y)/\partial y$ [V/m]
(f = 10 [MHz] and U = 10 [V])

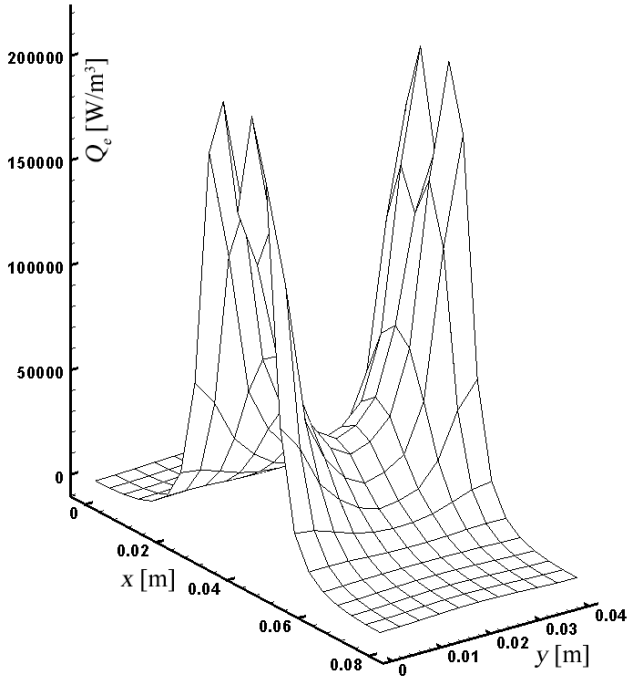

Fig. 10. Source function Q_e [W/m^3] due to electric field
(f = 10 [MHz] and U = 10 [V])

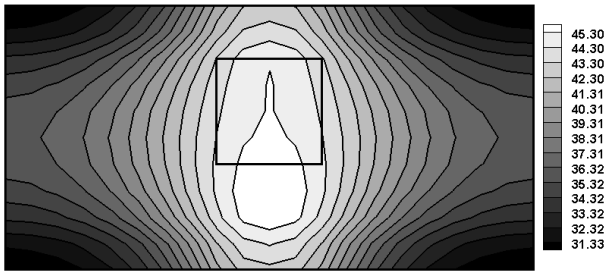

Fig. 11. Temperature distribution (α_w = 45 [W/(m^{2}K)],
T_w = 20 °C, f = 10 [MHz] and U = 10 [V])

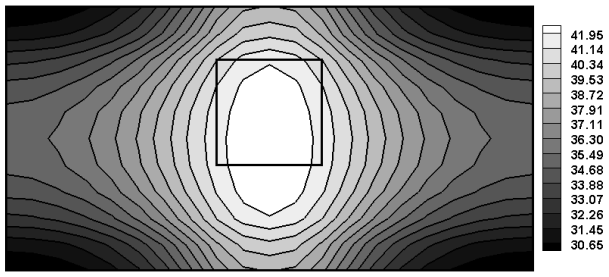

Fig. 12. Temperature distribution
(f = 0.1 [MHz] and U = 15 [V])

The maximum temperature lower than 42 °C does not always damage the tumor (rows 1, 2, 5 and 9 of the table). The optimal temperature distribution has been obtained for the input data collected in rows 3, 6, 10 of the table, being also represented in figures 12, 13, 11. The temperature distribution shown in figure 11 leads to the destruction of not only the tumor re-

gion, but also a large part of healthy tissue. On the other hand, the temperature distributions presented in figures 12 and 13 show that only a fragment of the tumor domain is destroyed.

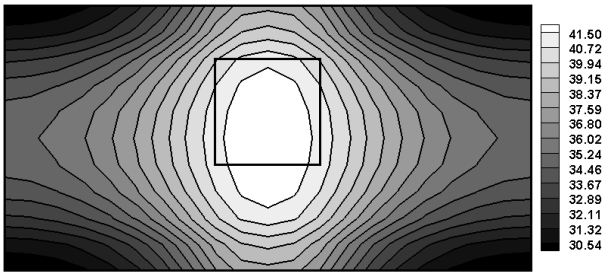

Fig. 13. Temperature distribution (f = 1 [MHz] and U = 10 [V])

The other input data from the table generate non-acceptable temperature fields (damage to the tumor and the healthy tissue). From the practical point of view, the choice of proper electric field parameters is difficult. Both the distance between the tumor and the skin surface and its dimensions should be taken into account. The conditions of skin surface cooling also play an essential role during the treatment by hyperthermia.

5. Conclusions

The boundary element method has been applied to solve the problem coupled with the biological tissue heating. The simplified 2D mathematical model based on the Pennes equation and supplemented with an equation determining the electric field generated by external electrodes is considered.

The potential φ (figure 7) has the largest gradients at the boundaries of electrodes (figures 8 and 9), therefore the source function Q_e due to electric field reaches the maximum in this area (figure 10). The changes of electric field parameters cause the changes of temperature in the entire domain considered, but the possibilities of controlling the temperature field (e.g. a concentration of maximum temperature at the central point of tumor region) are quite limited. Therefore, the concept of the introduction of micro/nanoparticles into the tumor region [2] (in order to concentrate energy at the cancerous tissue) seems to be very promising.

The method discussed can be applied, provided that the tumour site and its dimensions are perfectly well known. In such a case, the methods of numerical simulation are very effective tool allowing a proper choice of electric field parameters and cooling conditions on a skin surface. The model presented with the simplifications in the shape of tumor region and in the solution of 2D problem can be extended to more complex geometrical conditions.

Acknowledgement

This paper has been sponsored by the State Committee for Scientific Research, Grant No. N N501 3667 34.

References

[1] WANG H., DAI W., BEJAN A., *Optimal temperature distribution in a 3D triple-layered skin structure embedded with artery and vein vasculature and induced by electromagnetic radiation*, International Journal of Heat and Mass Transfer, 2007, 50, 1843–1854.

[2] LV Y.G., DENG Z.S., LIU J., *3D numerical study on the induced heating effects of embedded micro/nanoparticles on human body subject to external medical electromagnetic field*, IEEE Transactions on Nanobioscience, 2005, Vol. 4, No. 4, 284–294.

[3] TSUDA N., KURODA K., *An inverse method to optimize heating conditions in RF-Capacitive Hyperthermia*, IEEE Transactions on Biomedical Engineering, 1996, Vol. 43, No. 10, 1029–1037.

[4] ZHU L., XU L.X., CHENCINSKI N., *Quantification of the 3-D electromagnetic power absorption rate in tissue during transurethral prostatic microwave thermotherapy using heat transfer model*, IEEE Transactions on Biomedical Engineering, 1998, Vol. 45, No. 9, 1163–1172.

[5] MARTIN G.T., HADDAD M.G., CRAVALHO E.G., BOWMAN H.F., *Thermal model for the local microwave hyperthermia treatment of benign prostatic hyperplasia*, IEEE Transactions on Biomedical Engineering, 1992, Vol. 39, No. 8, 836–844.

[6] MARMOR J.B., POUNDS D., POSTIC T.B., HAHN G.M., *Treatment of superficial human neoplasms by hyperthermia induced by ultrasound*, Cancer, 1979, Vol. 43, 196–200.

[7] KIM B.M., JACQUES S.L., RASTEGAR S., THOMSEN S., MOTAMEDI M., *Nonlinear finite-element analysis of the role of dynamic changes in blood perfusion and optical properties in laser coagulation of tissue*, IEEE Journal of Selected Topics in Quantum Electronics, 1996, Vol. 2, No. 4, 922–933.

[8] LIU J., XU L.X., *Boundary information-based diagnostics on the thermal states of biological bodies*, International Journal of Heat and Mass Transfer, 2000, 43, 2827–2839.

[9] MAJCHRZAK E., MOCHNACKI B., *Analysis of thermal processes occurring in tissue with a tumor region using the BEM*, Journal of Theoretical and Applied Mechanics, 2002, 1, 40, 101–112.

[10] MOCHNACKI B., MAJCHRZAK E., *Sensitivity of the skin tissue on the activity of external heat sources*, Computer Modelling in Engineering and Sciences, 2003, Vol. 4, No. 3–4, 431–438.

[11] THIEBAUT C., LEMONNIER D., *Three-dimensional modelling and optimization of thermal fields in human body during hyperthermia*, International Journal of Thermal Sciences, 2002, 41, 500–508.

[12] TORVI D.A., DALE J.D., *A finite element model of skin subjected to a flash fire*, Journal of Mechanical Engineering, 1994, 116, 250–255.

[13] MAJCHRZAK E., JASIŃSKI M., *Numerical estimation of burn degree of skin tissue using the sensitivity analysis methods*, Acta of Bioengineering and Biomechanics, 2003, Vol. 5, No. 1, 93–108.

[14] BREBBIA C.A., DOMINGUEZ J., *Boundary elements, an introductory course*, Computational Mechanics Publications, McGraw-Hill Book Company, London, 1992.

[15] MAJCHRZAK E., *Boundary element method in heat transfer* (in Polish), publication of the Częstochowa University of Technology, Częstochowa, 2001.